Journal of Organometallic Chemistry 872 (2018) 114–122

Contents lists available at ScienceDirect

Journal of Organometallic Chemistry

journal homepage: www.elsevier.com/locate/jorganchem

Half-sandwich Ir(III) and Rh(III) 2,2′-dipyridylamine complexes: Synthesis, characterization and *in vitro* cytotoxicity against the ovarian carcinoma cells

Pavel Štarha, Zdeněk Dvořák, Zdeněk Trávníček*

Biologically Active Complexes and Molecular Magnets, Regional Centre of Advanced Technologies and Materials, Faculty of Science, Palacký University in Olomouc, Šlechtitelů 27, 783 71, Olomouc, Czech Republic

ARTICLE INFO

Article history:
Received 19 June 2018
Received in revised form
25 July 2018
Accepted 29 July 2018
Available online 1 August 2018

Keywords:
Iridium(III)
Rhodium(III)
Half-sandwich
2,2′-dipyridylamine
Crystal structure
Cytotoxicity

ABSTRACT

A series of the half-sandwich Ir(III) and Rh(III) complexes $[M(\eta^5\text{-}Cp^x)(dpa)X]PF_6$ (M = Ir for **1**–**6** and Rh for **7**–**12**) containing *N*-(pyridin-2-yl)pyridin-2-amine (2,2′-dipyridylamine, dpa), pentamethylcyclopentadienyl (Cp*; for **1**–**5** and **7**–**11**) or 1,2,3,4-tetramethyl-5-phenylcyclopentadienyl (Cp^{ph}; for **6** and **12**) ring, and various monodentate ligands (X), specifically Cl^- (for **1**, **6**, **7** and **12**), Br^- (for **2** and **8**), I^- (for **3** and **9**), valproato (VP; for **4** and **10**) or 4-phenylbutyrato (PB; for **5** and **11**), was prepared. The complexes were thoroughly characterized by elemental analysis, IR and NMR spectroscopy and mass spectrometry. A single-crystal X-ray analysis was performed for complex $[Ir(\eta^5\text{-}Cp^{ph})(dpa)Cl]PF_6$ (**6**), revealing a pseudo-octahedral piano-stool geometry with a bidentate *N,N′*-coordinated dpa ligand, a penta-hapto coordinated Cp^{ph} ring and a monodentate chlorido ligand. The crystal structure of complex **6** is stabilized by N–H···F, C–H···F, C–H···Cl, C–H···C and C···F non-covalent contacts. Complexes **1**–**12** were screened for their *in vitro* cytotoxicity against the A2780 human ovarian carcinoma cell line. The best-performing iridium(III) complex **6** showed markedly higher activity (IC_{50} = 23.5 μM) than complexes **1**–**3**, **5**, **9** and **12**, whose IC_{50} ranged from 68.7 to 87.1 μM. Iridium(III) complex **4** and rhodium(III) complexes **7**, **8**, **10** and **11** were inactive against the A2780 cells in the tested concentration range (IC_{50} > 100.0 μM). The chlorido complexes **1**, **6**, **7** and **12** were studied by ^{1}H NMR spectroscopy for their hydrolytic stability in the 20% DMF-d_7/80% D_2O and 20% MeOD-d_4/80% D_2O mixture of solvents, revealing Ir(III) complexes **1** and **6** as stable, while Rh(III) complexes **7** and **12** partially hydrolysed in the used medium. Moreover, hydrophobicity (lipophilicity) of complexes **1**–**12** was studied by an octanol/water partition (log*P*).

1. Introduction

In the last decade, various rhodium and iridium complexes have been reported as agents showing considerable cytotoxic activity against human cancer cells [1], thus representing an alternative for the conventional platinum-based drugs (*e.g.*, *cisplatin* or *oxaliplatin*), whose clinical application is connected with serious negative side-effects (*e.g.*, nephrotoxicity or myelosuppression) and problems with resistance [2]. Among them, Ir(III) and Rh(III) half-sandwich cyclopentadienyl (Cp) complexes of the $[M(\eta^5\text{-}Cp)(Y\hat{}Z)X]^{+/0}$ type seem to be a promising group of agents for the development of cytotoxic non-platinum complexes [1,3]; Y^Z = a bidentate-coordinated ligand, X = a monodentate (usually halogenido) ligand. These compounds offer a different mechanism of action than platinum-based drugs and a different cytotoxicity profile, resulting in their capability to overcome both the acquired and intrinsic resistance of cancer cells against the therapeutic action of platinum-based chemotherapeutics [3a,4].

From the structure-activity relationship point of view, it has been reported that cytotoxicity of Ir(III) half-sandwich complexes can be tuned by a Cp-ring extension. In particular, pentamethylcyclopentadienyl (Cp*) complexes, such as $[Ir(\eta^5\text{-}Cp^*)(phen)Cl]PF_6$ (IC_{50} > 100 μM), show lower anticancer potency than analogues containing extended Cp^{ph} (IC_{50} = 6.7 μM) and Cp^{bph} (IC_{50} = 0.7 μM) Cp-rings, studied at the A2780 human ovarian carcinoma cell line; Cp^{ph} = 1,2,3,4-tetramethyl-5-phenylcyclopentadienyl, Cp^{bph} = 1,2,3,4-tetramethyl-5-biphenylcyclopentadienyl, phen = 1,10-phenanthroline [5].

* Corresponding author.
E-mail address: zdenek.travnicek@upol.cz (Z. Trávníček).

https://doi.org/10.1016/j.jorganchem.2018.07.035
0022-328X/

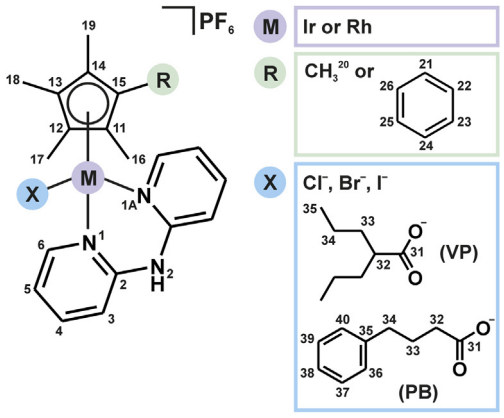

Complex	M	Cp^{x}	X
1	Ir	Cp*	Cl$^-$
2	Ir	Cp*	Br$^-$
3	Ir	Cp*	I$^-$
4	Ir	Cp*	VP
5	Ir	Cp*	PB
6	Ir	Cp^{ph}	Cl$^-$
7	Rh	Cp*	Cl$^-$
8	Rh	Cp*	Br$^-$
9	Rh	Cp*	I$^-$
10	Rh	Cp*	VP
11	Rh	Cp*	PB
12	Rh	Cp^{ph}	Cl$^-$

Fig. 1. A general structural formula of the studied iridium(III) and rhodium(III) complexes **1**–**12**, given together with the specifications of the Cp-ring substitution and type of the monodentate X ligand.

However, the same dependence was not observed for the Rh(III) analogues of the above-mentioned Ir(III) complexes, namely [Rh(η^5-Cp*)(phen)Cl]PF$_6$ (IC$_{50}$ = 17.8 μM), [Rh(η^5-Cp^{ph})(phen)Cl]PF$_6$ (IC$_{50}$ = 57.0 μM) and [Rh(η^5-Cp^{bph})(phen)Cl]PF$_6$ (IC$_{50}$ = 14.7 μM) [4].

Further, the replacement of the chlorido ligand of complexes [Ir(η^5-Cp)(Y^Z)Cl]$^{+/0}$ by a different type of a monodentate ligand, such as pyridine or its derivatives or hydrosulfide, leads to the cytotoxicity enhancement of the studied agents [6]. However, the effect of the replacement of the chlorido ligand by other halogenido ligands has not been performed yet for half-sandwich Ir(III) and Rh(III) complexes. It is noteworthy that these studies have been performed for half-sandwich Ru(II) and Os(II) complexes [7]. The reported results suggested that a relevant difference of cytotoxicity can be reached by the halogenido ligand variation, as exemplified on complexes [Ru(η^6-*p*cym)(L)Cl]PF$_6$ (IC$_{50}$ = 16.2 μM) *vs.* [Ru(η^6-*p*cym)(L)I]PF$_6$ (IC$_{50}$ = 3.0 μM), and [Os(η^6-*p*cym)(L)Cl]PF$_6$ (IC$_{50}$ = 3.0 μM) *vs.* [Os(η^6-*p*cym)(L)I]PF$_6$ (IC$_{50}$ = 1.2 μM); L = *N*,*N*-dimethyl-4-[(*E*)-pyridin-2-yl-diazenyl]-aniline [7a].

Another possibility how to tune the biological effect (cytotoxicity and/or processes connected with the mechanism of action) of [M(ar)(Y^Z)Cl]$^{+/0}$ half-sandwich complexes (ar = a five- or six-membered aromatic ring) can be based on the replacement of the chlorido ligand by the bioactive one, as recently reported by us [8] and others [9]. For example, complex [Ir(η^5-Cp^{ph})(phen)(PB)]PF$_6$, bearing the *O*-coordinated histone deacetylase inhibitor 4-phenylbutyrate (PB), showed a different cytotoxic profile (RF = 0.8) than its chlorido analogue [Ir(η^5-Cp^{ph})(phen)Cl]PF$_6$ (RF = 1.8); RF = IC$_{50}$(A2780R)/IC$_{50}$(A2780); A2780R is a *cisplatin*-resistant variant of the A2780 cells [8b].

In this work, we aimed to prepare a series of [Ir(η^5-Cp^{x})(dpa)X]PF$_6$ (**1**–**6**) and [Rh(η^5-Cp^{x})(dpa)X]PF$_6$ (**7**–**12**) complexes (Fig. 1) with different monodentate ligands (*i.e.*, Cl$^-$, Br$^-$, I$^-$, valproate (VP) and PB) and Cp-rings (Cp* and Cp^{ph}) and explore whether these structural variations affect the *in vitro* cytotoxicity against the A2780 human ovarian carcinoma cell line; dpa = *N*-(pyridin-2-yl) pyridin-2-amine (2,2′-dipyridylamine).

2. Experimental section

2.1. Materials

IrCl$_3\cdot n$H$_2$O and RhCl$_3\cdot n$H$_2$O were purchased from Precious Metals Online. 2,2′-dipyridylamine (dpa), 1,2,3,4,5-pentamethylcyclopentadiene, 2,3,4,5-tetramethyl-2-cyclopentenone, phenylmagnesium bromide (3.0 M in diethyl ether), MgSO$_4$, KBr, KI, valproic acid, 4-phenylbutyric acid, NaOH, silver trifluoromethanesulfonate (AgOTf), silver nitrate, KCl, NH$_4$PF$_6$ and *cisplatin* were purchased from Sigma-Aldrich, VWR International or Alfa Aesar Ltd. Solvents of a laboratory grade were purchased from Fisher-Scientific and Litolab, and used without further purification, except THF that was dried using 4 Å molecular sieves. DMSO-d_6, DMF-d_7, MeOD-d_4 and D$_2$O for NMR experiments were supplied by Sigma-Aldrich. Roswell Park Memorial Institute (RPMI-1640) medium, fetal bovine serum, glutamine, penicillin/streptomycin mixture, trypsin and phosphate-buffered saline (PBS) were purchased from Sigma-Aldrich and Fisher-Scientific.

The starting compounds [Ir(μ-Cl)(η^5-Cp*)Cl]$_2$ [10], [Ir(μ-Cl)(η^5-Cp^{ph})Cl]$_2$ [11], [Rh(μ-Cl)(η^5-Cp*)Cl]$_2$ [10], [Rh(μ-Cl)(η^5-Cp^{ph})Cl]$_2$ [4], silver valproate (AgVP) [12] and silver 4-phenylbutyrate (AgPB) [12] were prepared following the reported protocols.

2.2. Syntheses

2.2.1. Complex [Ir(η^5-Cp*)(dpa)Cl]PF$_6$ (**1**)

Complex **1** was prepared by the reaction of [Ir(μ-Cl)(η^5-Cp*)Cl]$_2$ (0.05 mmol) with dpa (0.10 mmol), stirred in MeOH (5 mL) at ambient temperature for 2 h, leading to a change from an orange suspension to a yellow solution containing complex [Ir(η^5-Cp*)(dpa)Cl]Cl (**1***). Then, an excess of NH$_4$PF$_6$ (0.25 mmol) was added and after 5 min of stirring at ambient temperature the reaction mixture was filtered and the solvent volume was reduced by nitrogen gas until a yellow product precipitated. Complex **1** was collected, washed (1 × 0.5 mL of MeOH and 3 × 1.0 mL of diethyl ether) and dried under vacuum.

Anal. Calcd. for IrC$_{20}$H$_{24}$N$_3$ClPF$_6$ (**1**): C, 35.37; H, 3.56; N, 6.19%; found: C, 35.42; H, 3.79; N, 6.15%. ^{1}H NMR (CDCl$_3$, ppm): δ 12.74 (s, N2–H, 1H), 8.27 (d, J_{H-H} = 6.4 Hz, C6–H, 2H), 8.22 (d, J_{H-H} = 8.3 Hz, C3–H, 2H), 7.74 (m, C4–H, 2H), 7.03 (t, J_{H-H} = 6.4 Hz, C5–H, 2H), 1.44 (s, C16–C20–H, 15H). ^{13}C NMR (DMSO-d_6, ppm): δ 153.1 (C2), 150.5 (C6), 140.1 (C4), 120.2 (C5), 116.4 (C3), 87.7 (C11–C15), 8.6 (C16–C20). ^{1}H NMR (DMSO-d_6, ppm): δ 10.98 (s, N2–H, 1H), 8.33 (d, J_{H-H} = 6.4 Hz, C6–H, 2H), 8.00 (t, J_{H-H} = 7.8 Hz, C4–H, 2H), 7.33 (d, J_{H-H} = 9.2 Hz, C3–H, 2H), 7.26 (t, J_{H-H} = 6.4 Hz, C5–H, 2H), 1.39 (s, C16–C20–H, 15H). ^{13}C NMR (DMSO-d_6, ppm): δ 152.1 (C6), 151.5 (C2), 141.1 (C4), 120.9 (C5), 114.2 (C3), 87.7 (C11–C15), 8.1 (C16–C20). ESI + MS (MeOH, *m/z*): 534.1 (calc. 534.1; 100%; [Ir(Cp*)(dpa)Cl]$^+$), 498.3 (calc. 498.2; 50%; [Ir(Cp*)(dpa$^-$)]$^+$). IR (ATR, *ν*, cm^{-1}): 444, 456, 535, 582, 622,651,672, 771, 823, 906, 1024, 1050, 1068, 1105, 1122, 1152, 1234, 1259, 1285, 1306, 1361, 1384, 1428, 1467, 1486, 1526, 1580, 1632, 2905, 2937, 3057, 3118, 3167, 3223, 3341.

2.2.2. Complexes [Ir(η⁵-Cp)(dpa)Br]PF₆ (**2**) and [Ir(η⁵-Cp*)(dpa)I]PF₆ (**3**)*

Nearly identical preparative procedures were used for the syntheses of both complexes. The reaction mixture containing complex **1*** (0.05 mmol; see above) and AgOTf (0.10 mmol) reacted at ambient temperature in the dark in 5 mL of MeOH for 1 h. The white precipitate of AgCl was removed providing a clear light yellow solution, to which an excess (0.10 mmol) of either KBr (for **2**) or KI (for **3**) was added. The reaction mixture got darker during 2 h of stirring at ambient temperature. After that, NH_4PF_6 (0.25 mmol) was added, stirred at ambient temperature for 5 min, filtered and the solvent was evaporated leading to the precipitation of a yellow product, which was removed, washed (1 × 0.5 mL of MeOH and 3 × 1.0 mL of diethyl ether) and dried under vacuum.

Anal. Calcd. for $IrC_{20}H_{24}N_3BrPF_6$ (**2**): C, 33.20; H, 3.34; N, 5.81%; found: C, 33.03; H, 3.18; N, 5.75%. ^{1}H NMR ($CDCl_3$, ppm): δ 9.09 (s, N2−H, 1H), 8.46 (d, J_{H-H} = 5.5 Hz, C6−H, 2H), 7.82 (t, J_{H-H} = 7.3 Hz, C4−H, 2H), 7.53 (d, J_{H-H} = 8.3 Hz, C3−H, 2H), 7.11 (t, J_{H-H} = 6.4 Hz, C5−H, 2H), 1.47 (s, C16−C20−H, 15H). ^{1}H NMR (DMSO-d_6, ppm): δ 10.95 (s, N2−H, 1H), 8.42 (d, J_{H-H} = 5.5 Hz, C6−H, 2H), 8.00 (t, J_{H-H} = 7.8 Hz, C4−H, 2H), 7.31 (d, J_{H-H} = 9.2 Hz, C3−H, 2H), 7.24 (d, J_{H-H} = 6.9 Hz, C5−H, 2H), 1.43 (s, C16−C20−H, 15H). ESI + MS (MeOH, *m/z*): 578.1 (calc. 578.1; 100%; [Ir(Cp*)(dpa)Br]$^+$), 498.3 (calc. 498.2; 25%; [Ir(Cp*)(dpa$^-$)]$^+$). IR (ATR, ν, cm^{-1}): 445, 534, 555, 634, 661, 708, 740, 769, 823, 882, 1030, 1081, 1127, 1164, 1212, 1232, 1291, 1315, 1353, 1378, 1434, 1469, 1491, 1523, 1584, 1627, 2925, 2967, 3065, 3142, 3204, 3249, 3359.

Anal. Calcd. for $IrC_{20}H_{24}N_3IPF_6$ (**3**): C, 31.18; H, 3.14; N, 5.45%; found: C, 30.81; H, 2.85; N, 5.05%. ^{1}H NMR ($CDCl_3$, ppm): δ 9.66 (s, N2−H, 1H), 8.59 (d, J_{H-H} = 6.4 Hz, C6−H, 2H), 7.80 (m, C4−H, 2H), 7.66 (d, J_{H-H} = 8.3 Hz, C3−H, 2H), 7.05 (t, J_{H-H} = 6.4 Hz, C5−H, 2H), 1.54 (s, C16−C20−H, 15H). ^{1}H NMR (DMSO-d_6, ppm): δ 10.97 (s, N2−H, 1H), 8.56 (d, J_{H-H} = 5.5 Hz, C6−H, 2H), 7.99 (t, J_{H-H} = 7.8 Hz, C4−H, 2H), 7.29 (d, J_{H-H} = 8.3 Hz, C3−H, 2H), 7.20 (d, J_{H-H} = 6.4 Hz, C5−H, 2H), 1.49 (s, C16−C20−H, 15H). ESI + MS (MeOH, *m/z*): 626.1 (calc. 626.1; 100%; [Ir(Cp*)(dpa)I]$^+$), 498.3 (calc. 498.2; 25%; [Ir(Cp*)(dpa$^-$)]$^+$). IR (ATR, ν, cm^{-1}): 446, 533, 554, 620, 634, 660, 706, 740, 767, 822, 880, 1029, 1066, 1080, 1127, 1164, 1211, 1231, 1266, 1291, 1314, 1354, 1380, 1433, 1469, 1490, 1523, 1584, 1627, 2924, 2966, 2981, 3028, 3063, 3139, 3204, 3249, 3361.

2.2.3. Complexes [Ir(η⁵-Cp)(dpa)(VP)]PF₆ (**4**) and [Ir(η⁵-Cp*)(dpa)(PB)]PF₆ (**5**)*

Complex **1** (0.05 mmol; see above) was dissolved in 10 mL of MeOH and 0.15 mmol of AgVP (for **4**) or AgPB (for **5**) was added. After 2 h of stirring at ambient temperature in the dark, a white solid (AgCl and unreacted silver carboxylates) was filtered off and an excess of NH_4PF_6 (0.25 mmol) was added. The mixture was stirred meanwhile the solvent volume was reduced by a nitrogen gas to *ca.* 1 mL. After that, an excess of diethyl ether (5 mL) was poured in, resulting in the precipitation of products. The obtained complexes **4** and **5** were collected by filtration, washed (1 × 0.5 mL of MeOH and 3 × 1.0 mL of diethyl ether) and dried under vacuum.

Anal. Calcd. for $IrC_{28}H_{39}N_3O_2PF_6$ (**4**): C, 42.74; H, 5.00; N, 5.34%; found: C, 42.28; H, 4.95; N, 5.09. ^{1}H NMR ($CDCl_3$, ppm): δ 8.80 (s, N2−H, 1H), 8.75 (d, J_{H-H} = 5.5 Hz, C6−H, 2H), 7.82 (m, C4−H, 2H), 7.55 (d, J_{H-H} = 8.3 Hz, C3−H, 2H), 7.12 (t, J_{H-H} = 6.4 Hz, C5−H, 2H), 2.29 (m, C32−H, 1H), 1.44 (s, C16−C20−H, C33−H, 17H), 1.30 (m, C33−H, 2H), 1.19 (m, C34−H, 4H), 0.79 (t, J_{H-H} = 7.3 Hz, C35−H, 6H). ^{1}H NMR (DMSO-d_6, ppm): δ 10.88 (s, N2−H, 1H), 8.68 (d, J_{H-H} = 5.5 Hz, C6−H, 2H), 8.01 (t, J_{H-H} = 7.8 Hz, C4−H, 2H), 7.36 (d, J_{H-H} = 8.3 Hz, C3−H, 2H), 7.28 (d, J_{H-H} = 5.9 Hz, C5−H, 2H), 2.13 (qui, J_{H-H} = 4.6 Hz, C32−H, 1H), 1.38 (s, C16−C20−H, 15H), 1.18 (m, C33−H, 4H), 1.08 (m, C34−H, 4H), 0.70 (t, J_{H-H} = 7.3 Hz, C35−H, 6H). ESI + MS (MeOH, *m/z*): 641.6 (calc. 642.3; 5%; [Ir(Cp*)(dpa)(VP)]$^+$), 498.3 (calc. 498.2; 100%; [Ir(Cp*)(dpa$^-$)]$^+$). IR (ATR, ν, cm^{-1}): 446, 556, 652, 674, 772, 830, 1025, 1038, 1117, 1158, 1235, 1284, 1312, 1350, 1370, 1394, 1433, 1445, 1474, 1489, 1535, 1578, 1591, 1618, 1650, 2870, 2930, 2983, 3078, 3192.

Anal. Calcd. for $IrC_{30}H_{35}N_3O_2PF_6$ (**5**): C, 44.66; H, 4.37; N, 5.21%; found: C, 44.76; H, 4.60; N, 5.31%. ^{1}H NMR ($CDCl_3$, ppm): δ 8.79 (m, N2−H, C6−H, 3H), 7.81 (t, J_{H-H} = 7.3 Hz, C4−H, 2H), 7.52 (d, J_{H-H} = 8.3 Hz, C3−H, 2H), 7.23 (m, C36−H, C40−H, 2H), 7.12 (m, C5−H, C37−H, C38−H, C39−H, 5H), 2.56 (t, J_{H-H} = 7.8 Hz, C32−H, 2H), 2.34 (t, J_{H-H} = 7.3 Hz, C34−H, 2H), 1.88 (qui, J_{H-H} = 7.8 Hz, C33−H, 2H), 1.43 (s, C16−C20−H, 15H). ^{1}H NMR (DMSO-d_6, ppm): δ 10.86 (N2−H, 1H), 8.75 (d, J_{H-H} = 5.9 Hz, C6−H, 2H), 8.00 (t, J_{H-H} = 7.8 Hz, C4−H, 2H), 7.35 (d, J_{H-H} = 8.6 Hz, C3−H, 2H), 7.28 (t, J_{H-H} = 6.5 Hz, C5−H, 2H), 7.14 (m, C37−H, C38−H, C39−H, 3H), 7.00 (m, C36−H, C40−H, 2H), 2.42 (t, J_{H-H} = 7.6 Hz, C32−H, 2H), 2.15 (t, J_{H-H} = 7.0 Hz, C34−H, 2H), 1.72 (t, J_{H-H} = 7.4 Hz, C33−H, 2H), 1.38 (s, C16−C20−H, 15H). ESI + MS (MeOH, *m/z*): 661.7 (calc. 662.2; 10%; [Ir(Cp*)(dpa)(PB)]$^+$), 498.3 (calc. 498.2; 100%; [Ir(Cp*)(dpa$^-$)]$^+$). IR (ATR, ν, cm^{-1}): 449, 470, 515, 555, 621, 650, 670, 701, 728, 772, 830, 878, 909, 968, 1028, 1082, 1161, 1186, 1240, 1268, 1314, 1329, 1358, 1380, 1435, 1468, 1490, 1535, 1576, 1590, 1618, 1643, 2789, 2840, 2865, 2928, 2953, 3064, 3088, 3183, 3289, 3372.

*2.2.4. Complex [Ir(η⁵-Cp^{ph})(dpa)Cl]PF₆ (**6**)*

The preparation of complex **6** was similar to that of complex **1**, except that [Ir(μ-Cl)(η⁵-Cp^{ph})Cl]$_2$ was used instead of [Ir(μ-Cl)(η⁵-Cp*)Cl]$_2$, and the reaction was performed in the microwave reaction system (100 °C, 1 min). *Anal.* Calcd. for $IrC_{25}H_{26}N_3ClPF_6$ (**6**): C, 40.51; H, 3.54; N, 5.67%; found: C, 40.38; H, 3.67; N, 5.42%. ^{1}H NMR ($CDCl_3$, ppm): δ 8.92 (s, N2−H, 1H), 8.34 (d, J_{H-H} = 5.5 Hz, C6−H, 2H), 7.78 (m, C4−H, 2H), 7.60 (m, Cp$^{ph}_{arom.}$, 2H), 7.52 (d, J_{H-H} = 9.2 Hz, C3−H, 2H), 7.48 (m, Cp$^{ph}_{arom.}$, 3H), 7.01 (t, J_{H-H} = 6.9 Hz, C5−H, 2H), 1.53 (s, Cp$^{ph}_{aliph.}$, 6H), 1.48 (s, Cp$^{ph}_{aliph.}$, 6H). ^{1}H NMR (DMSO-d_6, ppm): δ 11.05 (s, N2−H, 1H), 8.30 (d, J_{H-H} = 5.9 Hz, C6−H, 2H), 7.98 (t, J_{H-H} = 7.7 Hz, C4−H, 2H), 7.57 (m, Cp$^{ph}_{arom.}$, 2H), 7.47 (m, Cp$^{ph}_{arom.}$, 3H), 7.34 (d, J_{H-H} = 8.8 Hz, C3−H, 2H), 7.19 (t, J_{H-H} = 6.6 Hz, C5−H, 2H), 1.48 (s, Cp$^{ph}_{aliph.}$, 6H), 1.41 (s, Cp$^{ph}_{aliph.}$, 6H). ESI + MS (MeOH, *m/z*): 596.1 (calc. 596.1; 100%; [Ir(Cp^{ph})(dpa)Cl]$^+$), 560.2 (calc. 560.2; 60%; [Ir(Cp^{ph})(dpa$^-$)]$^+$). IR (ATR, ν, cm^{-1}): 446, 461, 531, 553, 583, 618, 705, 744, 758, 774, 823, 905, 929, 1006, 1031, 1064, 1101, 1128, 1165, 1211, 1236, 1266, 1352, 1380, 1448, 1471, 1521, 1585, 1628, 2919, 2964, 2984, 3063, 3119, 3397.

Single-crystals of complex **6** suitable for an X-ray analysis were obtained from the mother liquor after 24 h of standing at ambient temperature.

*2.2.5. Rh(III) complexes **7**–**11***

The preparation of complexes [Rh(η⁵-Cp*)(dpa)Cl]PF₆ (**7**), [Rh(η⁵-Cp*)(dpa)Br]PF₆ (**8**), [Rh(η⁵-Cp*)(dpa)I]PF₆ (**9**), [Rh(η⁵-Cp*)(dpa)(VP)]PF₆ (**10**) and [Rh(η⁵-Cp*)(dpa)(PB)]PF₆ (**11**) were similar to those of their Ir(III) analogues **1**–**5**, except that [Rh(μ-Cl)(η⁵-Cp*)Cl]$_2$ was used instead of [Ir(μ-Cl)(η⁵-Cp*)Cl]$_2$.

Anal. Calcd. for $RhC_{20}H_{24}N_3ClPF_6$ (**7**): C, 40.73; H, 4.10; N, 7.13%; found: C, 40.70; H, 3.99; N, 7.01%. ^{1}H NMR ($CDCl_3$, ppm): δ 9.07 (s, N2−H, 1H), 8.39 (d, J_{H-H} = 5.5 Hz, C6−H, 2H), 7.87 (t, J_{H-H} = 7.8 Hz, C4−H, 2H), 7.53 (d, J_{H-H} = 8.3 Hz, C3−H, 2H), 7.21 (d, J_{H-H} = 6.4 Hz, C5−H, 2H), 1.49 (s, C16−C20−H, 15H). ^{1}H NMR (DMSO-d_6, ppm): δ 10.94 (s, N2−H, 1H), 8.35 (d, J_{H-H} = 5.5 Hz, C6−H, 2H), 8.03 (t, J_{H-H} = 7.3 Hz, C4−H, 2H), 7.33 (m, C3−H, C5−H, 4H), 1.41 (s, C16−C20−H, 15H). ESI + MS (MeOH, *m/z*): 444.0 (calc. 444.1; 80%; [Rh(Cp*)(dpa)Cl]$^+$), 408.2 (calc. 408.1; 100%; [Rh(Cp*)(dpa$^-$)]$^+$). IR (ATR, ν, cm^{-1}): 444, 535, 554, 623, 658, 708, 741, 772, 821, 883, 1024, 1081, 1126, 1165, 1209, 1233, 1317, 1351, 1376, 1434, 1466, 1489, 1520, 1583, 1625, 2925, 2968, 2990, 3065, 3105, 3141, 3205, 3246, 3364.

Anal. Calcd. for $RhC_{20}H_{24}N_3BrPF_6$ (**8**): C, 37.88; H, 3.81; N, 6.63%; found: C, 37.67; H, 3.93; N, 6.63%. ^{1}H NMR ($CDCl_3$, ppm): δ 9.30 (s, N2–H, 1H), 8.47 (d, J_{H-H} = 4.6 Hz, C6–H, 2H), 7.85 (t, J_{H-H} = 7.8 Hz, C4–H, 2H), 7.54 (d, J_{H-H} = 8.3 Hz, C3–H, 2H), 7.17 (t, J_{H-H} = 6.4 Hz, C5–H, 2H), 1.52 (s, C16–C20–H, 15H). ^{1}H NMR (DMSO-d_6, ppm): δ 10.95 (s, N2–H, 1H), 8.42 (d, J_{H-H} = 4.6 Hz, C6–H, 2H), 8.03 (t, J_{H-H} = 7.8 Hz, C4–H, 2H), 7.31 (m, C3–H, C5–H, 4H), 1.46 (s, C16–C20–H, 15H). ESI + MS (MeOH, *m/z*): 488.0 (calc. 488.0; 100%; $[Rh(Cp^*)(dpa)Br]^+$), 408.1 (calc. 408.1; 60%; $[Rh(Cp^*)(dpa^-)]^+$). IR (ATR, ν, cm^{-1}): 443, 534, 554, 633, 658, 707, 741, 770, 821, 882, 904, 1023, 1080, 1126, 1163, 1232, 1291, 1317, 1351, 1376, 1433, 1467, 1522, 1552, 1583, 1625, 2925, 2968, 2988, 3064, 3137, 3196, 3230, 3277, 3365.

Anal. Calcd. for $RhC_{20}H_{24}N_3IPF_6$ (**9**): C, 35.26; H, 3.55; N, 6.17%; found: C, 35.07; H, 3.80; N, 6.21%. ^{1}H NMR ($CDCl_3$, ppm): δ 9.87 (s, N2–H, 1H), 8.58 (d, J_{H-H} = 4.6 Hz, C6–H, 2H), 7.83 (m, C4–H, 2H), 7.77 (d, J_{H-H} = 8.3 Hz, C3–H, 2H), 7.12 (d, J_{H-H} = 6.4 Hz, C5–H, 2H), 1.60 (s, C16–C20–H, 15H). ^{1}H NMR (DMSO-d_6, ppm): δ 10.97 (s, N2–H, 1H), 8.54 (d, J_{H-H} = 5.5 Hz, C6–H, 2H), 8.02 (t, J_{H-H} = 7.8 Hz, C4–H, 2H), 7.28 (m, C3–H, C5–H, 4H), 1.55 (s, C16–C20–H, 15H). ESI + MS (MeOH, *m/z*): 536.0 (calc. 536.0; 100%; $[Rh(Cp^*)(dpa)I]^+$), 408.1 (calc. 408.1; 10%; $[Rh(Cp^*)(dpa^-)]^+$). IR (ATR, ν, cm^{-1}): 445, 533, 555, 622, 740, 772, 831, 871, 904, 1021, 1079, 1123, 1161, 1233, 1265, 1357, 1379, 1433, 1468, 1521, 1554, 1583, 1625, 2915, 2963, 2985, 3024, 3073, 3128, 3195, 3229, 3272, 3377.

Anal. Calcd. for $RhC_{28}H_{39}N_3O_2PF_6$ (**10**): C, 48.22; H, 5.64; N, 6.02%; found: C, 48.53; H, 5.32; N, 6.16%. ^{1}H NMR ($CDCl_3$, ppm): δ 8.84 (d, J_{H-H} = 5.5 Hz, C6–H, 2H), 8.81 (s, N2–H, 1H), 7.85 (m, C4–H, 2H), 7.48 (d, J_{H-H} = 8.3 Hz, C3–H, 2H), 7.20 (t, J_{H-H} = 6.4 Hz, C5–H, 2H), 2.28 (m, C32–H, 1H), 1.46 (m, C16–C20–H, C33–H, 17H), 1.29 (m, C33–H, 2H), 1.18 (m, C34–H, 4H), 0.77 (t, J_{H-H} = 7.3 Hz, C35–H, 6H). ^{1}H NMR (DMSO-d_6, ppm): δ 10.89 (s, N2–H, 1H), 8.76 (d, J_{H-H} = 5.5 Hz, C6–H, 2H), 8.04 (t, J_{H-H} = 7.3 Hz, C4–H, 2H), 7.36 (m, C3–H, C5–H, 4H), 2.10 (qui, J_{H-H} = 4.6 Hz, C32–H, 1H), 1.38 (s, C16–C20–H, 15H), 1.17 (m, C33–H, 4H), 1.08 (m, C34–H, 4H), 0.69 (t, J_{H-H} = 7.3 Hz, C35–H, 6H). ESI + MS (MeOH, *m/z*): 551.7 (calc. 552.2; 5%; $[Rh(Cp^*)(dpa)(VP)]^+$), 408.2 (calc. 408.1; 100%; $[Rh(Cp^*)(dpa^-)]^+$). IR (ATR, ν, cm^{-1}): 451, 555, 587, 652, 671, 775, 828, 1022, 1065, 1116, 1157, 1223, 1246, 1280, 1313, 1367, 1396, 1419, 1433, 1454, 1477, 1489, 1537, 1557, 1595, 1615, 1656, 2873, 2932, 2956, 3079, 3194.

Anal. Calcd. for $RhC_{30}H_{35}N_3O_2PF_6$ (**11**): C, 50.22; H, 4.92; N, 5.86%; found: C, 50.31; H, 4.68; N, 5.49%. ^{1}H NMR ($CDCl_3$, ppm): δ 8.87 (m, N2–H, C6–H, 3H), 7.85 (m, C4–H, 2H), 7.47 (d, J_{H-H} = 8.3 Hz, C3–H, 2H), 7.18 (m, C36–C40–H, 5H), 7.09 (d, J_{H-H} = 7.3 Hz, C5–H, 2H), 2.56 (t, J_{H-H} = 7.8 Hz, C32–H, 2H), 2.32 (t, J_{H-H} = 7.8 Hz, C34–H, 2H), 1.89 (qui, J_{H-H} = 7.8 Hz, C33–H, 2H), 1.43 (s, C16–C20–H, 15H). ^{1}H NMR (DMSO-d_6, ppm): δ 10.90 (N2–H, 1H), 8.83 (d, J_{H-H} = 5.5 Hz, C6–H, 2H), 8.03 (t, J_{H-H} = 7.3 Hz, C4–H, 2H), 7.35 (m, C3–H, C5–H, 4H), 7.17 (m, C37–H, C38–H, C39–H, 3H), 7.01 (d, J_{H-H} = 7.3 Hz, C36–H, C40–H, 2H), 2.42 (t, J_{H-H} = 7.3 Hz, C32–H, 2H), 2.11 (t, J_{H-H} = 6.9 Hz, C34–H, 2H), 1.72 (m, C33–H, 2H), 1.38 (s, C16–C20–H, 15H). ESI + MS (MeOH, *m/z*): 517.5 (calc. 572.2; 5%; $[Rh(Cp^*)(dpa)(PB)]^+$), 408.1 (calc. 408.1; 100%; $[Rh(Cp^*)(dpa^-)]^+$). IR (ATR, ν, cm^{-1}): 445, 472, 555, 645, 700, 745, 775, 830, 877, 1026, 1080, 1163, 1237, 1273, 1309, 1360, 1395, 1435, 1471, 1533, 1568, 1585, 1630, 1645, 2818, 2857, 2930, 2962, 3084, 3186, 3295, 3374.

2.2.6. Complex $[Rh(\eta^5\text{-}Cp^{ph})(dpa)Cl]PF_6$ (**12**)

Complex **12** was prepared similarly as described above for complex **6**, using $[Rh(\mu\text{-}Cl)(\eta^5\text{-}Cp^{ph})Cl]_2$ instead of $[Ir(\mu\text{-}Cl)(\eta^5\text{-}Cp^{ph})Cl]_2$. *Anal.* Calcd. for $RhC_{25}H_{26}N_3ClPF_6$ (**12**): C, 46.07; H, 4.02; N, 6.45%; found: C, 46.25; H, 3.93; N, 6.37%. ^{1}H NMR ($CDCl_3$, ppm): δ 8.89 (s, N2–H, 1H), 8.34 (d, J_{H-H} = 6.4 Hz, C6–H, 2H), 7.75 (m, C4–H, 2H), 7.64 (m, $Cp^{ph}_{arom.}$, 2H), 7.54 (d, J_{H-H} = 8.3 Hz, C3–H, 2H), 7.49 (m, $Cp^{ph}_{arom.}$, 3H), 7.04 (t, J_{H-H} = 6.9 Hz, C5–H, 2H), 1.54 (s, $Cp^{ph}_{aliph.}$, 6H), 1.46 (s, $Cp^{ph}_{aliph.}$, 6H). ^{1}H NMR (DMSO-d_6, ppm): δ 11.01 (s, N2–H, 1H), 8.30 (d, J_{H-H} = 5.9 Hz, C6–H, 2H), 8.00 (t, J_{H-H} = 7.7 Hz, C4–H, 2H), 7.67 (d, J_{H-H} = 6.6 Hz, $Cp^{ph}_{arom.}$, 2H), 7.51 (m, $Cp^{ph}_{arom.}$, 3H), 7.33 (d, J_{H-H} = 8.1 Hz, C3–H, 2H), 7.23 (t, J_{H-H} = 6.6 Hz, C5–H, 2H), 1.48 (s, $Cp^{ph}_{aliph.}$, 6H), 1.45 (s, $Cp^{ph}_{aliph.}$, 6H). ESI + MS (MeOH, *m/z*): 505.9 (calc. 506.1; 70%; $[Rh(Cp^{ph})(dpa)Cl]^+$), 470.1 (calc. 470.1; 100%; $[Rh(Cp^{ph})(dpa^-)]^+$). IR (ATR, ν, cm^{-1}): 444, 475, 534, 554, 706, 738, 771, 819, 883, 1023, 1081, 1125, 1164, 1208, 1233, 1284, 1351, 1378, 1432, 1466, 1520, 1583, 1624, 2924, 2968, 3065, 3141, 3322, 3364.

2.3. General methods

^{1}H NMR spectra were recorded using a JEOL JNM-ECA 600II device on $CDCl_3$ and DMSO-d_6 solutions of complexes **1**–**12** at 300 K, supported by ^{13}C, ^{1}H–^{1}H gs-COSY, ^{1}H–^{13}C gs-HMQC and ^{1}H–^{13}C gs-HMBC spectra of complex **1**; gs = gradient selected, COSY = correlation spectroscopy, HMQC = heteronuclear multiple quantum coherence, HMBC = heteronuclear multiple bond coherence. ^{1}H and ^{13}C NMR spectra were calibrated against the residual signals of the used solvents found at 7.26 ppm (^{1}H) and 77.4 (^{13}C) for $CDCl_3$, and at 2.50 ppm (^{1}H) and 39.5 ppm (^{13}C) for DMSO-d_6 solutions [13]. The splitting of proton resonances in the reported ^{1}H spectra is defined as s = singlet, d = doublet, t = triplet, qui = quintet, m = multiplet. Electrospray ionization mass spectrometry (ESI-MS) was performed by an LCQ Fleet ion trap spectrometer (Thermo Scientific; QualBrowser software, version 2.0.7) in the positive ionization mode (ESI+) on the methanolic solutions of the studied complexes. Elemental analyses (C, H, N) were carried out using a Flash 2000 CHNS Elemental Analyser (Thermo Scientific). Infrared spectroscopy (400–4000 cm^{-1}, Attenuated total reflectance (ATR) technique) was performed by a Nexus 670 FT-IR spectrometer (Thermo Fisher Scientific).

2.4. X-ray crystallography

The X-ray diffraction data of complex $[Ir(\eta^5\text{-}Cp^{ph})(dpa)Cl]PF_6$ (**6**) were collected by a Bruker D8 QUEST diffractometer (Mo Kα radiation) equipped with a PHOTON 100 CMOS detector. The obtained data were processed and reduced by the APEX3 software package [14] and the molecular structure of complex **6** was solved by direct methods (SHELXS) and refined by a full-matrix least-squares procedure (SHELXL) [15]. Hydrogen atoms of all the structures were found in the difference Fourier maps and refined using a riding model with C–H = 0.95 Å for $(CH)_{aromatic}$ and 0.98 Å for (CH_3), and with $U_{iso}(H) = 1.2\ U_{eq}(CH)$ and $1.5\ U_{eq}(CH_3)$. The X-ray crystallographic data for complex **6** have been deposited in the Cambridge Crystallographic Data Centre under the accession number CCDC 1849574. The crystal data and structure refinements are given in Table 1. The graphics were drawn and additional structural calculations were performed by DIAMOND [16] and Mercury [17] software.

2.5. In vitro cytotoxicity testing

An appropriate amount of complexes **1**–**12** was dissolved in 500 μL of DMF to give the stock solutions of the 100 mM concentration. The stock solutions were diluted by RPMI-1640 medium to the concentrations of 0.1–100.0 μM.

The A2780 human ovarian carcinoma cell line (supplied by European Collection of Cell Cultures, ECACC) was cultured according to the ECACC instructions, *i.e.*, as adherent monolayers in a humidified atmosphere (37 °C, 5% CO_2), in RPMI-1640 medium

Table 1
Crystal data and structure refinement for [Ir(η^5-Cp^{ph})(dpa)Cl]PF_6 (**6**).

Empirical formula	$C_{25}H_{26}ClIrN_3 \cdot F_6P$
Formula weight	741.11
Temperature (K)	120(2)
Wavelength (Å)	0.71073
Crystal system	Monoclinic
Space group	$P2_1/n$
Unit cell dimensions	
a (Å)	14.689(3)
b (Å)	10.770 (2)
c (Å)	16.714 (3)
α (°)	90
β (°)	104.179(9)
γ (°)	90
V (Å^3)	2563.7(8)
Z, D_{calc} (g cm^{-3})	4, 1.920
Absorption coefficient (mm^{-1})	5.439
Crystal size (mm)	0.22 × 0.16 × 0.14
F (000)	1440
θ range for data collection (°)	2.271 to 27.560
Index ranges (h, k, l)	$-19 \le h \le 19$ $-14 \le k \le 14$ $-21 \le l \le 21$
Reflections collected	63423
Independent reflections	5903, R(int) = 0.0491
Data/restraints/parameters	5903/0/341
Goodness–of–fit on F^2	1.045
Final R indices [$I > 2\sigma(I)$]	$R_1 = 0.0212$, w$R_2 = 0.0433$
R indices (all data)	$R_1 = 0.0295$, w$R_2 = 0.0461$
Largest peak and hole (e Å^{-3})	1.052 and −1.112

supplemented with 10% of fetal calf serum, 1% of 2 mM glutamine and 1% penicillin/streptomycin. The cells were seeded to 96-well culture plates, preincubated in drug-free media at 37 °C for 24 h and treated with complexes **1**–**12** (and *cisplatin* involved as the reference drug). After 24 h drug exposure, the supernatants were removed and the cells were washed with drug-free PBS followed by 72 h recovery in a drug-free medium at 37 °C. In parallel, the cells were also treated with 0.1% DMF and 1% Triton X-100 to assess the minimal (*i.e*, 100% cell viability for negative control) and maximal (*i.e*, 0% cell viability for positive control) cell damage, respectively. The MTT assay (MTT = 3-(4,5-dimethylthiazol-2-yl)-2,5-diphenyltetrazolium bromide) was used to determine the cell viability. A concentration of the formed dye was evaluated spectrophotometrically at 540 nm (TECAN, Schoeller Instruments LLC).

The data from the cancer cells were acquired from three independent experiments (conducted in triplicate) using the cells from different passages. The data were expressed as the percentage of viability and the resulting IC_{50} values (μM), calculated from the viability curves, are given as arithmetic mean ± SD.

2.6. ^{1}H NMR studies of hydrolytic stability

The MeOD-d_4 solutions (120 μL) were prepared from 0.81 mg (for **1**), 0.89 mg (for **6**), 0.71 mg (for **7**) and 0.78 mg (for **12**) of the studied chlorido complexes and 480 μL of D_2O was added to each solution to provide 600 μL of 2 mM solutions in 20% MeOD-d_4/80% D_2O. ^{1}H NMR spectra were acquired on the fresh solutions ($t \approx 0$ h) and after 1, 2, 6, 24 and 48 h of standing at ambient temperature. Spectra were calibrated against the residual solvent signal of methanol (3.34 ppm) [13]. After 48 h of standing at ambient temperature, an excess (5 mol equiv.) of KCl was added to the equilibrated solutions of complexes **1**, **6**, **7** and **12** in 20% MeOD-d_4/80% D_2O and ^{1}H NMR spectra were recorded. For comparative purposes, ^{1}H NMR spectra were also acquired for the **1^h**, **6^h**, **7^h** and **12^h** species in the same medium, which were prepared from the fresh solutions of complexes **1**, **6**, **7** and **12** in 20% MeOD-d_4/80% D_2O by the addition of the stoichiometric amount of silver nitrate. The mixtures were shaken under an aluminium foil (25 °C) for 1 h, then the formed precipitate of AgCl was centrifuged and the obtained solutions were used for ^{1}H NMR experiments. The same experiments were carried out for complexes **1**, **6**, **7** and **12** in 20% DMF-d_7/80% D_2O mixture of solvents. Spectra were calibrated against the residual solvent signal of DMF (8.03 ppm) [13].

^{1}H NMR experiments at different pH were performed for Rh(III) complexes **7** and **12** to determine the composition of their hydrolysates (*i.e*., aqua *vs*. hydroxido species). The solutions of the **7^h** and **12^h** species were performed in 5% MeOD-d_4/95% D_2O (*note:* solubility of complexes **7** and **12** in D_2O was under the detection limit of the used device). pH* was adjusted by $DClO_4$ and KOD solutions (0.1, 0.01 and 0.001 M) to the values of 4, 7 and 10 and ^{1} H NMR spectra were recorded at the individual pH* points (pH* = pH in D_2O).

2.7. Hydrophobicity studies

Octanol-saturated water (OSW) and water-saturated octanol (WSO) were prepared from octanol and 0.2 M water solution of KCl (for chlorido complexes **1**, **6**, **7** and **12**), KBr (for bromido complexes **2** and **8**), KI (for iodido complexes **3** and **9**), NaVP (for valproato complexes **4** and **10**) or NaPB (for 4-phenylbutyrato complexes **5** and **11**) by the overnight stirring. The stock solutions were prepared by shaking (Vibramax 100, Heidolph Instruments) of 1 μmol of complexes **1**–**12** in 11 mL of OSW for 1 h. Then the mixtures were centrifuged (5 min, 11,000 rpm) and supernatant was collected. 5 mL of this solution was studied by ICP-MS (the obtained values were corrected for the adsorption effects) for the Ir or Rh content (*e.g.*, [M]OSW_b, see below), while other 5 mL of this solution was added to 5 mL of WSO and shaken for 2 h at ambient temperature. After that, these mixtures were centrifuged and aqueous layers were carefully separated. The Ir or Rh concentrations were determined by ICP-MS (the obtained value was corrected for the adsorption effects). log$P$ = log([M]WSO/[M]OSW_a) equation was used for the partition coefficient calculation; [M]OSW_b and [M]OSW_a stands for the Ir or Rh concentration before and after partition, respectively, and [M]WSO = [M]OSW_b − [M]OSW_a. The experiment was conducted in triplicate and the results are presented as arithmetic mean ± SD.

3. Results and discussion

3.1. Synthesis and general characterization

In this work, a series of ionic iridium(III) (**1**–**6**) and rhodium(III) (**7**–**12**) complexes of the general composition [M(η^5-Cp^x)(dpa)X]PF_6 was studied (Fig. 1). The herein used chelating *N,N*-donor dpa ligand is a known organic ligand offering various coordination modes [18], and it has recently been reported as a chelating ligand of complexes [M(η^5-Cp*)(dpa)Cl]Cl·2H_2O (M = Ir or Rh), representing the hydrated chloride salts of complexes **1** and **7** reported herein [19].

Chlorido complexes **1**, **6**, **7** and **12** were prepared according the conventional protocol widely used for similar half-sandwich Ir(III) and Rh(III) complexes, which uses the dimeric compounds [M(μ-Cl)(η^5-Cp^x)Cl]$_2$ (M = Ir or Rh, Cp^x = Cp* or Cp^{ph}) as the Ir(III) and Rh(III) starting materials (*e.g.*, ref. [3,4]). The [Ir(η^5-Cp*)(dpa)Cl]$^+$ and [Rh(η^5-Cp*)(dpa)Cl]$^+$ species, representing the cations of complexes **1** and **7**, were recently prepared by the same method (but in dichloromethane with markedly longer reaction time of 16 h) as employed in this work, and isolated as the hydrated chloride salts [Ir(η^5-Cp*)(dpa)Cl]Cl·2H_2O and [Rh(η^5-Cp*)(dpa)Cl]Cl·2H_2O [19]. Bromido (**2**, **8**) and iodido **3**, **9**) complexes were

prepared from the $[Ir(\eta^5\text{-}Cp^*)(dpa)Cl]^+$ chlorido species through their dechlorination by AgOTf, followed by the addition of appropriate potassium halogenide. The syntheses of carboxylato complexes **4**, **5**, **10** and **11** were similar to those recently reported for the half-sandwich complexes $[Os(\eta^6\text{-}p\text{cym})(dpa)(VP)]PF_6$ [8a], $[Ir(\eta^5\text{-}Cp^{ph})(phen)(PB)]PF_6$ [8b], $[Ru(\eta^6\text{-}p\text{cym})(dpa)(VP)]PF_6$ and $[Ru(\eta^6\text{-}p\text{cym})(dpa)(PB)]PF_6$ [12].

The purity and composition of complexes **1**–**12** (Fig. 1) were studied by elemental analysis (<0.4% differences between the theoretical and experimental C, H, and N contents), ^{1}H NMR spectroscopy, ESI + mass spectrometry and FTIR spectroscopy. The infrared spectra of complexes **1**–**12** showed the peaks of the characteristic vibrations of the Cp^x ligand at 2905–2990 (for $\nu_s(C\text{–}H)_{aliphatic}$ and $\nu_{as}(C\text{–}H)_{aliphatic}$) and at 1440–1470 and *ca* 770 cm^{-1} for $\nu_{as}(C\text{–}C)$, and $\nu_{as}(C\text{–}CH_3)$, respectively [19,20]. The peaks at 3030–3200 cm^{-1} belong to the $\nu(C\text{–}H)_{aromatic}$ vibrations of the dpa (for **1**–**12**) and Cp^{ph} (for **6** and **12**) ligands. Further for the dpa ligand, the peaks centred around 3350 cm^{-1} are assignable to the ν(N–H) vibration [19,21]. For carboxylato complexes **4**, **5**, **10** and **11**, the characteristic peaks belonging to the ν_{as}(C=O) and ν_s(C=O) vibrations were observed at *ca* 1645, and 1390 cm^{-1}, respectively, for the VP and PB ligands [22]. The FTIR spectra of all complexes contained the peaks assignable to the ν(P–F) vibrations of the PF_6^- counterion centred at *ca.* 830, 770 and 555 cm^{-1} [23].

ESI + mass spectra showed the peaks of the $[M(Cp^x)(dpa)X]^+$ species, corresponding to the cations of the studied complexes **1**–**12**, and the $[M(Cp^x)(dpa^-)]^+$ species, which formed from the complex cations of complexes **1**–**12** by a release of the corresponding halogenido or carboxylato ligand (X) together with a proton (most likely from the –NH group of the dpa ligand).

All the signals of both Cp^x and dpa ligands were detected in ^{1}H NMR spectra of complexes **1**–**12** dissolved in $CDCl_3$ (Figs. S1–S7) and DMSO-d_6. For example, the characteristic N2–H singlet of the dpa ligand was detected at 8.79–12.74 ppm (for $CDCl_3$ solutions) and at 10.86–11.05 ppm (for DMSO-d_6 solutions). The aromatic C–H signals of the dpa ligand showed between 8.87 and 7.01 ppm (for $CDCl_3$ solutions). Moreover, ^{1}H NMR spectra of carboxylato complexes **4**, **5**, **10** and **11** (both $CDCl_3$ and DMSO-d_6 solutions) revealed the signals of the VP and PB ligands, such as the C_α–H (*i.e.*, C32–H) signal detected for VP at *ca* 2.10 ppm (for complexes **4** and **10**) and for PB at 2.42 ppm (for complexes **5** and **11**). Further for the carboxylato complexes **4**, **5**, **10** and **11** (both $CDCl_3$ and DMSO-d_6 solutions), the δ values of the VP and PB ligands differ markedly from free valproate (*e.g.*, $\delta = 2.39$ ppm ($CDCl_3$) and 2.21 ppm (DMSO-d_6) for C32–H) and 4-phenylbutyrate anions (*e.g.*, $\delta = 2.68$ ppm ($CDCl_3$) and 2.53 ppm (DMSO-d_6) for C32–H) (Fig. S8). The chemical shifts of the dpa, VP and PB ligands were consistent with the values observed for complexes $[Os(\eta^6\text{-}p\text{cym})(dpa)(VP)]PF_6$ [8a], $[Ru(\eta^6\text{-}p\text{cym})(dpa)(VP)]PF_6$ and $[Ru(\eta^6\text{-}p\text{cym})(dpa)(PB)]PF_6$ [12].

The presence of the Cp* ligand in the structure of complexes **1**–**5** and **7**–**11** was proved by its characteristic ^{1}H NMR singlet detected at 1.43–1.60 (for $CDCl_3$ solutions) and at 1.38–1.55 ppm (for DMSO-d_6 solutions), while ^{1}H NMR spectra of Cp^{ph}-complexes **6** and **12** contain two singlets 1.46–1.54 (for $CDCl_3$ solutions) and 1.41–1.48 ppm for DMSO-d_6 solutions) in the aliphatic region, belonging to the C16–C19 methyl groups (see Fig. 1). The ^{1}H NMR studies revealed that complexes **1**–**12** are stable in the $CDCl_3$ and DMSO-d_6 solution, because no chemical shift changes and/or new signals were detected after 72 h of standing at ambient temperature.

3.2. X-ray structure of complex **6**

The crystallographically characterized complex $[Ir(\eta^5\text{-}Cp^{ph})(dpa)Cl]PF_6$ (**6**) adopts a pseudo-octahedral piano-stool coordination geometry, a typical one for similar cyclopentadienyl half-sandwich Ir(III) complexes (Fig. 2). The central Ir(III) atom is coordinated by the extended cyclopentadienyl ring (Cp^{ph}), chlorido ligand and by two nitrogen atoms (*i.e*, N(1) and N(1A)) of the bidentate-coordinated dpa ligand. The determined bond lengths and angles around the central Ir(III) atom are summarized in Table 2.

Complex **6** is structurally similar to the previously reported Cp^{ph} complexes $[Ir(\eta^5\text{-}Cp^{ph})(phen)Cl]PF_6$ (CCDC 802288), $[Ir(\eta^5\text{-}Cp^{ph})(bpy)Cl]PF_6$ (CCDC 802287) and $[Ir(\eta^5\text{-}Cp^{ph})(en)Cl]BPh_4$ (CCDC 802290), which represent the only three deposited X-ray structures of Ir(III) chlorido complexes containing the Cp^{ph} ring and a chelating *N,N*-donor ligand; bpy = 2,2′-bipyridyl, en = ethylene-1,2-diamine [3a]. The Ir–Cl and Ir–N bond lengths of complex **6** (Table 2) are comparable with those detected for three above-mentioned X-ray structures of similar Ir(III) half-sandwich Cp^{ph} complexes, for which the average values equalled 2.395(11) Å (for Ir–Cl bond) and 2.10(2) Å (for Ir–N bonds). Also of interest for cyclopentadienyl half-sandwich complexes, the Ir–Cg distance in complex **6** (Table 2) falls into the range of 1.7827–1.7945 Å reported for the Ir(III) Cp^{ph} chlorido complexes containing phen, bpy and en [3a].

The dihedral angle between both pyridines of the dpa ligand equals 33.75(9)°, which is somehow higher than 28.00(7)° calculated for the Rh(III) complex $[Rh(\eta^5\text{-}Cp^*)(dpa)Cl]Cl\cdot 2H_2O$ (CCDC 1012354) [19]. Another intraligand dihedral angle of complex **6** is formed by the cyclopentadienyl ring and its phenyl substituent and its value is 54.12(10)°. Concerning the interligand dihedral angles between the cyclopentadienyl ring and both pyridines of dpa, they were calculated as 21.53(11)° (for the *N*(1)-containing pyridine ring) and 23.64(10)° (for the *N*(1A)-containing pyridine ring).

As for the molecular structure of the cationic complex **6** (Fig. S9 and Table S1), it also contains the PF_6^- anion, with the shortest Ir···P distance of 6.038(2) Å for Ir···P(1)^{vii} (symmetry code: vii, -x, 1-y, 1-z), connected with the complex cation *via* N–H···F, C–H···F and C···F non-covalent intermolecular contacts. In addition, there are also C–H···Cl contacts between the dpa and chlorido ligands of the adjacent complex cations stabilizing the crystal structure, and intermolecular C–H···C contacts detected between the Cp^{ph} and dpa ligands (see Table S1). The shortest Ir···Ir distance is 7.1049(10) for Ir···Ir^v (symmetry code: v, 1-x, -y, 1-z).

3.3. In vitro cytotoxicity testing

In vitro cytotoxicity of complexes **1**–**12** was studied against the

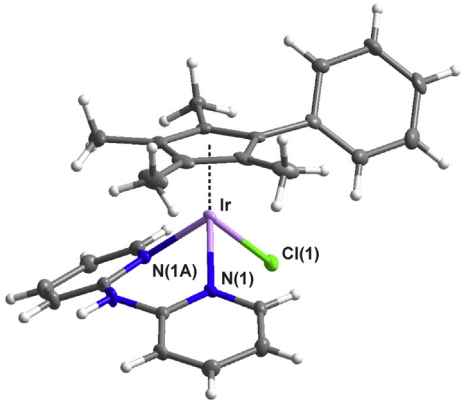

Fig. 2. The molecular structure of complex $[Ir(\eta^5\text{-}Cp^{ph})(dpa)Cl]PF_6$ (**6**) showing the atom labelling scheme. Displacement ellipsoids are drawn at the 50% probability level.

Table 2
Selected bond lengths (Å) and angles (°) determined by a single-crystal X-ray analysis for complex [Ir(η^5-Cp^{ph})(dpa)Cl]PF$_6$ (**6**). Cg = centroid of the cyclopentadienyl ring of the Cp^{ph} ligand.

Bond lengths (Å)		Bond angles (°)	
Ir–N(1)	2.101(2)	N(1)–Ir–N(1A)	83.63(9)
Ir–N(1A)	2.097(2)	N(1)–Ir–Cl(1)	87.52(6)
Ir–Cl(1)	2.3877(7)	N(1)–Ir–Cg	126.52(7)
Ir–C(20)	2.186(3)	N(1A)–Ir–Cl(1)	85.30(6)
Ir–C(21)	2.151(3)	N(1A)–Ir–Cg	126.93(7)
Ir–C(22)	2.159(3)	Cl(1)–Ir–Cg	131.44(2)
Ir–C(23)	2.157(3)	C(2)–N(2)–C(2)A	126.1(2)
Ir–C(24)	2.177(3)		
Ir–Cg	1.7858(4)		

A2780 human ovarian carcinoma cells, which were treated by the studied agents for 24 h, followed by 72 h recovery time in a drug-free medium. The A2780 cell viability was evaluated by an MTT assay, providing the cell viability curves, from which the resulting IC_{50} values were calculated (see Table 3).

The obtained results indicated that Ir(III) chlorido complexes **1** and **6** are markedly more *in vitro* cytotoxic than their Rh(III) analogues **7** and **12**. Importantly, the impact of the Cp-ring extension from Cp* (complexes **1** and **7**) to Cp^{ph} (complexes **6** and **12**) on the *in vitro* cytotoxicity was positive in the case of both Ir(III) and Rh(III) pairs of agents. The replacement of the chlorido ligand by different halogenido ones did not led to any general trend of *in vitro* cytotoxicity. In particular, Ir(III) complexes **2** and **3** were less potent than chlorido complex **1**, while Rh(III) iodido complex **9** exceeded the biological effect of both its halogenido analogues **7** and **8**. It is noteworthy, that Rh(III) iodido complex **9** showed comparable cytotoxicity with Ir(III) chlorido complex **1**. Concerning the carboxylato complexes, they were (complexes **4**, **10** and **11**) inactive up to the highest tested concentration in most cases, meaning that in the case of Ir(III) complexes the replacement of the chlorido ligand of complex **1** by the VP one (complex **4**) caused a decrease of *in vitro* cytotoxicity against the A2780 cells. PB complex **5** was comparably cytotoxic with complex **1** against the A2780 cells, which is consistent with the results observed for a pair of chlorido and 4-phenylbutyrato complexes [Ir(η^5-Cp^{ph})(phen)Cl]PF$_6$ and [Ir(η^5-Cp^{ph})(phen)(PB)]PF$_6$, studied at the same human cancer cells [8].

All the complexes, including the best-performing complex **6**, were less cytotoxic than the reference-drug *cisplatin* ($IC_{50} = 5.9 \pm 1.2$ μM) and the relative activity (RA) of complex **6** equalled *ca.* 0.3, which is comparable with the formerly reported Cp^{ph} complex [Ir(η^5-Cp^{ph})(phen)Cl]PF$_6$ (RA ~ 0.2) [3a,5], and slightly higher than for [Ir(η^5-Cp^{ph})(bpy)Cl]PF$_6$ (RA ~ 0.1) [3a,5] and the clinically investigated Ru(III) complex KP1019 (RA ~ 0.1) [24], studied at the same human cancer cells against *cisplatin* as the reference. A superior cytotoxicity of Ir(III) complex within pairs of analogical Ir(III) and Rh(III) chlorido complexes, as observed for Cp* complexes **1** and **7**, and Cp^{ph} complexes **6** and **12** in this work, was also reported for a pair of half-sandwich Cp* Ir(III) and Rh(III) complexes containing 1,3,5-tris(di-2-pyridylaminomethyl)benzene [25]. In particular, RA of these agents equals *ca.* 0.5 (for Ir(III) complex) and *ca.* 0.9 (for Rh(III) complex) at ovarian carcinoma cells (*cisplatin* was used as a reference drug). Further, in contrast to complexes **7** and **12** (see Table 3), Cp^{ph} complex [Rh(η^5-Cp^{ph})(phen)Cl]PF$_6$ (IC_{50} = 57.0 μM) was less cytotoxic than its Cp* analogue [Rh(η^5-Cp*)(phen)Cl]PF$_6$ (IC_{50} = 17.8 μM) at A2780 cells [4].

3.4. ^{1}H NMR studies of hydrolytic stability

Because chlorido complexes **1**, **6**, **7** and **12** were the most cytotoxic type of the studied iridium(III) and rhodium(III) complexes (except for the inactive complex **7** involved in the hydrolysis studies for comparative purposes), their hydrolytic stability in water-containing media (20% DMF-d_7/80% D_2O and 20% MeOD-d_4/80% D_2O) was studied by ^{1}H NMR; *note:* DMF-d_7 and MeOD-d_4 ensured the dissolution of low water-soluble complexes in the sufficient concentration (i.e. 2 mM).

^{1}H NMR spectra of the best-performing complex **1** and **6** did not change in time in both the used mixtures of solvents (Fig. 3 and Fig. S10). In particular, only one set of the C–H signals of dpa was detected at 8.47 (C6–H), 8.05 (C4–H), 7.43 (C3–H) and 7.37 (C5–H) ppm in the spectra acquired for complex **1** on the fresh 20% DMF-d_7/80% D_2O solution and after 48 h of standing at ambient temperature (Fig. 3). The position of the ^{1}H NMR signals detected in the spectra of complex **1** did not change even after the addition of excess KCl (5 mol equiv.), proving these complexes as hydrolytically stable under the used conditions (Fig. 3). This is also evidenced by a difference in the signal positions of complex **1** in comparison with its dechlorinated species **1^h** (Table 4 and Fig. 3). The same was observed also for hydrolytically stable complex **1**, whose ^{1}H NMR spectra in 20% DMF-d_7/80% D_2O contained only one set of signals (even after 48 h of standing at 25 °C) with different δ values than observed for **1^h** (Table 4).

In contrast to the above discussed iridium(III) chlorido complexes **1** and **6**, their rhodium(III) analogues **7** and **12** hydrolysed rapidly, which is evidenced by the presence of two sets of ^{1}H NMR signals of both dpa and Cp^x (Cp^x = Cp* for **7** or Cp^{ph} for **12**) ligands detected in their spectra (Table 4, Fig. 3 and Fig. S10), as observed in both the used water-containing media. The hydrolysis rate of *ca.* 30% (for **7**) and *ca.* 25% (for **12**) detected on the fresh 20% DMF-d_7/80% D_2O solution did not change in time up to 48 h of standing at

Table 3
The results of *in vitro* cytotoxicity (IC_{50}±SD; μM) of [M(η^5-Cp^x)(dpa)X]PF$_6$ complexes **1**–**12** against the A2780 human ovarian carcinoma cells treated for 24 h followed by 72 h recovery in a drug-free media, given together with log*P* values of complexes **1**–**12**.

X	Cp^x	M = Ir	IC_{50} (μM)	log*P*	M = Rh	IC_{50} (μM)	log*P*
Cl	Cp*	**1**	70.6 ± 2.6	−0.52 ± 0.09	**7**	>100.0	−1.45 ± 0.05
Br	Cp*	**2**	87.1 ± 5.3	−0.29 ± 0.03	**8**	>100.0	−0.35 ± 0.02
I	Cp*	**3**	83.0 ± 4.1	1.69 ± 0.03	**9**	70.1 ± 4.6	1.29 ± 0.03
VP	Cp*	**4**	>100.0	−0.19 ± 0.01	**10**	>100.0	−1.87 ± 0.00
PB	Cp*	**5**	76.9 ± 11.4	−0.17 ± 0.02	**11**	>100.0	−1.52 ± 0.19
Cl	Cp^{ph}	**6**	23.5 ± 1.1	0.37.±0.02	**12**	68.7 ± 7.2	−1.31 ± 0.15

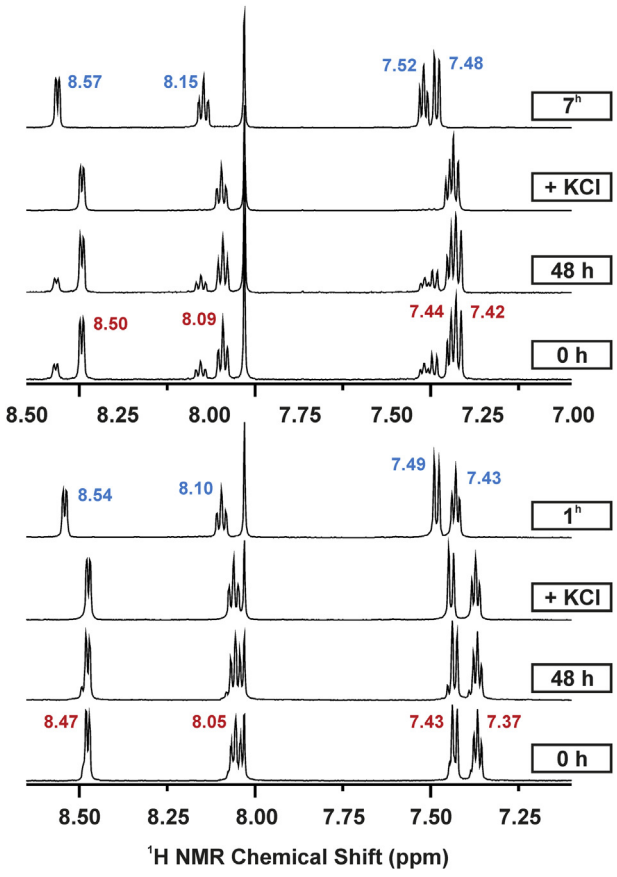

Fig. 3. ^{1}H NMR studies of the representative complexes **1** and **7** in 20% DMF-d_7/80% D_2O, as observed at different time points (t = 0 or 48 h) and at various conditions (+KCl stands for the addition of 5 M equiv. of KCl). Spectra of the dechlorinated species $\mathbf{1^h}$ and $\mathbf{7^h}$ were depicted as well for comparative purposes.

ambient temperature. As a consequence of the addition of excess KCl, one set of signals disappeared in the ^{1}H NMR spectra of complexes **7** and **12** (with δ corresponding to the dechlorinated species $\mathbf{7^h}$ and $\mathbf{12^h}$, respectively). Thus, the signals remaining in the spectra after the KCl addition can be unambiguously assigned to the studied chlorido complexes (Table 4, Fig. 3 and Fig. S10).

The formation of the hydroxido species rather than the aqua ones was proved for complexes **7** and **12** by the results of pH*-dependent ^{1}H NMR experiments, because the same chemical shifts were observed for the dechlorinated species at pH* = equal to 7 and 10 (*e.g.*, 8.36 and 7.96 ppm for C6–H, and C4–H, respectively, for complex $\mathbf{12^h}$), while the δ values changed as a consequence of pH* decrease to 4 (*e.g.*, 8.43 and 8.04 ppm for C6–H and C4–H, respectively) [4].

3.5. Hydrophobicity studies

Hydrophobicity (lipophilicity) is an important feature of cytotoxic complexes known to be related to cellular accumulation and cytotoxicity itself. In this work, the log*P* values were determined by an octanol/water partition (Table 3). The obtained results showed, that iridium(III) complexes are more lipophilic than their rhodium(III) analogues. Unfortunately, no general conclusion can be drawn as for the comparison of lipophilicity and cytotoxicity. However, it can be seen in the case of iridium(III) complexes **1** and **6** that the Cp^{ph} chlorido complex **6** was more lipophilic than its Cp^* analogue **1**, which correlates with a higher anticancer potency of complex **6** over complex **1**. Similar trend of lipophilicity and cytotoxicity of iridium(III) Cp^{ph} and Cp^* complexes was reported for structurally very close complexes containing 1,10-phenanthroline or deprotonated 2-phenylpyridine [3a]. On the other hand, similar log*P* values were found in the case of rhodium(III) chlorido complexes **7** and **12**, although they differ in cytotoxicity. Moreover, the following trend in lipophilicity of halogenido Cp^* complexes **1**–**3** and **7**–**9** was observed for both iridium(III) and rhodium(III) complexes: I > Br > Cl. However, in the case of iridium(III) complexes, the least lipophilic complex **1** exceeded cytotoxicity of more lipophilic complexes **2** and **3**.

4. Conclusions

A series of iridium(III) and rhodium(III) $[M(\eta^5\text{-}Cp^x)(dpa)X]PF_6$ complexes **1**–**12** containing 2,2′-dipyridylamine (dpa), a variously substituted cyclopentadienyl ring (Cp^* or Cp^{ph}), and halogenido or carboxylato monodentate ligands (X) was synthesized and thoroughly characterized. The crystallographically characterized complex $[Ir(\eta^5\text{-}Cp^{ph})(dpa)Cl]PF_6$ (**6**) adopted a pseudo-octahedral piano-stool geometry, a typical one for similar half-sandwich complexes. Complexes **1**–**3**, **5**, **6**, **9** and **12** showed moderate

Table 4
The chemical shifts (in ppm) of the C–H signals of the dpa ligand, as observed by ^{1}H NMR spectroscopy on the fresh solutions (t = 0 h) of the chlorido complexes **1**, **6**, **7** and **12** in 20% DMF-d_7/80% D_2O or 20% MeOD-d_4/80% D_2O and after 48 h of standing at ambient temperature. For comparative purposes, the results acquired after the addition of excess KCl (labelled as "+ KCl") and the results obtained for the dechlorinated species $\mathbf{1^h}$, $\mathbf{6^h}$, $\mathbf{7^h}$ and $\mathbf{12^h}$ in the same medium are given as well.

Sample	20% DMF-d_7/80% D_2O						20% MeOD-d_4/80% D_2O					
	C3–H	C4–H	C5–H	C6–H	Content		C3–H	C4–H	C5–H	C6–H	Content	
					0 h	48 h					0 h	48 h
1	7.43	8.05	7.37	8.47	100%	100%	7.32	7.95	7.25	8.38	100%	100%
1 (+KCl)	7.44	8.06	7.37	8.48			7.32	7.95	7.25	8.38		
$\mathbf{1^h}$	7.49	8.10	7.43	8.54			7.40	8.02	7.30	8.42		
6	7.44	8.04	7.27	8.47	100%	100%	7.33	7.93	7.15	8.35	100%	100%
6 (+KCl)	7.46	8.05	7.28	8.47			7.33	7.93	7.15	8.35		
$\mathbf{6^h}$	7.50	8.09	7.34	8.52			7.40	8.00	7.24	8.43		
7	7.42	8.09	7.44	8.50	70%	70%	7.30	7.98	7.33	8.40	75%	75%
	7.49	8.15	7.52	8.57	30%	30%	7.35	8.05	7.38	8.45	25%	25%
7 (+KCl)	7.43	8.10	7.45	8.50			7.31	7.99	7.33	8.41		
$\mathbf{7^h}$	7.48	8.15	7.52	8.57			7.35	8.04	7.38	8.45		
12	7.42	8.06	7.32	8.47	75%	75%	7.32	7.96	7.20	8.36	80%	80%
	7.49	8.13	7.42	8.55	25%	25%	7.37	8.02	7.30	8.42	20%	20%
12 (+KCl)	7.43	8.06	7.33	8.47			7.32	7.96	7.20	8.36		
$\mathbf{12^h}$	7.49	8.14	7.43	8.55			7.38	8.03	7.31	8.42		

in vitro cytotoxicity at the A2780 human ovarian carcinoma cells ($IC_{50} = 23.5–87.1$ μM). The obtained cytotoxicity results suggest that the replacement of the chlorido ligand of half-sandwich iridium(III) and rhodium(III) complexes by a different halogenido ligand (Br, I) or by a simple releasable bioactive *O*-donor ligand (valproato or 4-phenylbutyrato) has, in most cases, a negligible impact on the resulting potency of such agents. On the other hand, the positive effect of an extension of the cyclopentadienyl ring on *in vitro* cytotoxicity, recently reported for iridium(III) complexes, can be also accepted for half-sandwich rhodium(III) complexes, because complex [Rh(η^5-Cp^{ph})(dpa)Cl]PF_6 (**12**; $IC_{50} = 68.7$ μM) exceeds *in vitro* cytotoxicity of its Cp* analogue **7** ($IC_{50} > 100$ μM) at A2780 human cancer cells.

Notes

Conflicts of interest

None.

Acknowledgements

The authors gratefully thank the Ministry of Education, Youth and Sports of the Czech Republic (projects LO1305 and CZ.1.05/2.1.00/19.0377), the Czech Science Foundation (GAČR 17-08512Y) and Palacký University Olomouc (PrF_2018_011) for the financial support. The authors also thank Ms. Lucie Hanousková for her help with syntheses of complexes **1**–**12**, Ms. Kateřina Kubešová for *in vitro* cytotoxicity testing, Dr. Peter Antal for recording the NMR spectra, Assoc. Prof. Ján Vančo for performing ICP-MS experiments, Dr. Bohuslav Drahoš for recording the ESI-MS spectra, Mrs. Pavla Richterová for performing elemental analyses and Dr. Alena Klanicová for recording the FTIR spectra.

Appendix A. Supplementary data

CCDC 1849574 contains the supplementary crystallographic data for this paper, and these data can be obtained free of charge from The Cambridge Crystallographic Data Centre *via* https://www.ccdc.cam.ac.uk.

Supplementary data related to this article can be found at https://doi.org/10.1016.

Appendix B. Supplementary data

Supplementary data related to this article can be found at https://doi.org/10.1016/j.jorganchem.2018.07.035.

References

[1] C.H. Leung, H.J. Zhong, D.S.H. Chan, D.L. Ma, Coord. Chem. Rev. 257 (2013) 1764–1776.
[2] L. Kelland, Nat. Rev. Canc. 7 (2007) 573–584.
[3] (a) Z. Liu, P.J. Sadler, Acc. Chem. Res. 47 (2014) 1174–1185;
(b) J. Ruiz, V. Rodríguez, N. Cutillas, K.G. Samper, M. Capdevila, O. Palacios, A. Espinosa, Dalton Trans. 41 (2012) 12847–12856;
(c) P. Zhang, P.J. Sadler, J. Organomet. Chem. 839 (2017) 5–14;
(d) C.C. Konkankit, S.C. Marker, K.M. Knopf, J.J. Wilson, Dalton Trans. (2018), https://doi.org/10.1039/C8DT01858H. Advance Article.
[4] J.J. Soldevila-Barreda, A. Habtemariam, I. Romero-Canelón, P.J. Sadler, J. Inorg. Biochem. 153 (2015) 322–333.
[5] Z. Liu, A. Habtemariam, A.M. Pizarro, S.A. Fletcher, A. Kisova, O. Vrana, L. Salassa, P.C.A. Bruijnincx, G.J. Clarkson, V. Brabec, P.J. Sadler, J. Med. Chem. 54 (2011) 3011–3026.
[6] (a) Z. Liu, I. Romero-Canelón, A. Habtemariam, G.J. Clarkson, P.J. Sadler, Organometallics 33 (2014) 5324–5333;
(b) P. Štarha, A. Habtemariam, I. Romero-Canelón, G.J. Clarkson, P.J. Sadler, Inorg. Chem. 55 (2016) 2324–2331.
[7] (a) I. Romero-Canelón, L. Salassa, P.J. Sadler, J. Med. Chem. 56 (2013) 1291–1300;
(b) M. Kubanik, H. Holtkamp, T. Sohnel, S.M.F. Jamieson, C.G. Hartinger, Organometallics 34 (2015) 5658–5668.
[8] (a) P. Štarha, Z. Trávníček, R. Herchel, P. Jewula, Z. Dvořák, Dalton Trans. 47 (2018) 5714–5724;
(b) P. Štarha, Z. Trávníček, B. Drahoš, R. Herchel, Z. Dvořák, Appl. Organomet. Chem. 32 (2018) e4246;
(c) P. Štarha, Z. Trávníček, J. Vančo, Z. Dvořák, Molecules 23 (2018) 420.
[9] G. Agonigi, T. Riedel, M.P. Gay, L. Biancalana, E. Oñate, P.J. Dyson, G. Pampaloni, E. Paunescu, M.A. Esteruelas, F. Marchetti, Organometallics 35 (2016) 1046–1056.
[10] J. Tönnemann, J. Risse, Z. Grote, R. Scopelliti, K. Severin, Eur. J. Inorg. Chem. 2013 (2013) 4558–4562.
[11] D.M. Morris, M. McGeagh, D. De Peña, J.S. Merola, Polyhedron 84 (2014) 120–135.
[12] P. Štarha, Z. Trávníček, R. Křikavová, Z. Dvořák, Molecules 21 (2016) 1725.
[13] H.E. Gottlieb, V. Kotlyar, A. Nudelman, J. Org. Chem. 62 (1997) 7512–7515.
[14] Apex3, Bruker AXS Inc, Madison, WI, 2015.
[15] G.M. Sheldrick, Acta Crystallogr. C71 (2015) 3–8.
[16] K. Brandenburg, Diamond Version 4.0.3, Crystal Impact GbR, Bonn, Germany, 2015.
[17] C.F. Macrae, I.J. Bruno, J.A. Chisholm, P.R. Edgington, P. McCabe, E. Pidcock, L. Rodriguez-Monge, R. Taylor, J. van de Streek, P.A. Wood, J. Appl. Crystallogr. 41 (2008) 466–470.
[18] D.W. Brogden, J.F. Berry, Comments Mod. Chem. 36 (2016) 17–37.
[19] P.A. Vekariya, P.S. Karia, J.V. Vaghasiya, S. Soni, E. Suresh, M.N. Patel, Polyhedron 110 (2016) 73–84.
[20] E. Bencze, B.V. Lokshin, J. Mink, W.A. Herrmann, F.E. Kühn, J. Organomet. Chem. 55 (2001) 55–66.
[21] C.J. Pouchert, The Aldrich Library of Infrared Spectra (Ed. III), Aldrich Chemical Co., Milwaukee, WI, USA, 1981.
[22] (a) H.G. Brittain, Cryst. Growth Des. 10 (2010) 1990–2003;
(b) G. Petruševski, P. Naumov, G. Jovanovski, G. Bogoeva-Gaceva, S.W. Ng, ChemMedChem 3 (2008) 1377–1386.
[23] P. Govindaswamy, Y.A. Mozharivskyj, M.R. Kollipara, Polyhedron 24 (2005) 1710–1716.
[24] M. Groessl, O. Zava, P.J. Dyson, Metall 3 (2011) 591–599.
[25] A.B.P. Rao, A. Uma, T. Chiranjeevi, M.S. Bethu, J.V. Rao, D.K. Deb, B. Sarkar, W. Kaminsky, M.K. Rao, J. Organomet. Chem. 824 (2016) 131–139.